ISSN 0031-918X, Physics of Metals and Metallography, 2022, Vol. 123, No. 11, pp. 1084–1090. © Pleiades Publishing, Ltd., 2022.
Russian Text © The Author(s), 2022, published in Fizika Metallov i Metallovedenie, 2022, Vol. 123, No. 11, pp. 1153–1160.

ELECTRICAL AND MAGNETIC PROPERTIES

Characteristics of Angular Dependences of Parameters of Ferromagnetic and Spin-Wave Resonance Spectra of Magnetic Films

I. G. Vazhenina[a, b, *], R. S. Iskhakov[a], and V. Yu. Yakovchuk[a]

[a] *Kirensky Institute of Physics, Federal Research Center KSC SB RAS, Krasnoyarsk, 660036 Russia*
[b] *Siberian Federal University, Krasnoyarsk, 660041 Russia*
**e-mail: irina-vazhenina@mail.ru*

Received September 4, 2022; revised September 25, 2022; accepted September 29, 2022

Abstract—This paper presents the results of measuring the main parameters of the ferromagnetic and spin-wave resonance spectra (resonant field, linewidth, and intensity) of single-layer permalloy films at various angles in the out-of-plane orientation. The effect of the type of surface conditions on the angular dependence of the intensity ratio of adjacent modes is studied. A correspondence is established between the angle of the applied constant magnetic field with respect to the normal to the film and the change in the oscillation type from uniform to nonuniform. The revealed features of the angular dependences of the resonant field and the intensity of the spectral peak can be successfully used in the identification of microwave spectra. The fundamental magnetic parameters (effective magnetization, exchange interaction constant, surface anisotropy constant, and perpendicular anisotropy field) were determined.

Keywords: spin-wave and ferromagnetic resonance, surface anisotropy constant, thin magnetic films, boundary conditions

DOI: 10.1134/S0031918X2260124X

INTRODUCTION

Ferromagnetic (FMR) and spin-wave (SWR) resonances are dynamic methods for studying magnetic systems when determining the main magnetic parameters: the effective magnetization M_{eff}, the magnetic anisotropy constant, the exchange interaction constant A, and surface anisotropy constant K_S. The morphology of objects and classes of substances to which these techniques can be applied is very wide: thin ferromagnetic films [1–6], powder systems [7, 8], dilute magnetic semiconductors [9–11], and ferromagnetic metal–dielectric nanocomposites (granular alloys) [12, 13], as well as ferrihydride nanoparticles of chemical and biological origin [14, 15]. The advantages of FMR and SWR are the ease of measurements and the possibility of obtaining magnetostructural data on the objects under study [5, 16–18]. The reliability of the parameter determination depends on the accuracy of mode identification in the recorded microwave spectrum: their resonant field H_{res}, linewidths ΔH, and intensity I.

The interpretation of the peak in the microwave spectrum also determines the form of the dispersion relation $\omega_0 \sim H_{\text{res}}$ (where ω_0 is the resonant frequency and H_{res} is the resonant field) and the need to take into account certain anisotropic or morphological ($\Sigma N_i = 4\pi$) contributions in it. Unsuccessful attempts to describe the first recorded FMR spectrum [19, 20] by the dispersion relation $\omega_L = \gamma H_{\text{res}}$ (where ω_L is the Larmor frequency) are of interest in this case. The fundamental results of the theoretical description of FMR experiments for two orientations of an external field relative to the basis of the sample were obtained by Kittel [21, 22], where, in addition to the internal magnetic field H_0 of the sample, demagnetizing fields of form anisotropy are taken into account. More data on the contribution of various sources of anisotropy in FMR measurements can be obtained both by changing the orientation of the sample relative to the direction of an external magnetic field and by a complete frequency-field analysis.

New challenges arose in determining the conditions for the excitation of nonuniform magnetization modes in a thin ferromagnetic film in the form of exchange standing spin waves and their theoretical description [23, 24]. The main results of this stage in the development of the SWR and FMR methods are the range of film thicknesses (100–500 nm) in which the conditions for the excitation of coherent spin waves occur, the imposition of additional (exchange) boundary conditions on the film surface [24–26], and

the form of the dependence of the resonant fields on the mode number ($H_n \sim n^2$).

The relevance of this work is determined by the need to accurately determine the magnetic parameters of ultrathin magnetic structures (the thickness of the magnetic region smaller than 100 nm), which are used in low-dimensional devices. When using such structures, two main factors should be taken into account: the equivalence of the surface and bulk effects and the magnetization reorientation rate. The damping of the magnetization precession with respect to the equilibrium state can be determined from the FMR line width. The surface mode detected under certain conditions in the SWR spectrum makes it possible to determine the magnitude and sign of the surface anisotropy constant. We note that the microwave spectra of ultrathin films have some specific features ignoring of which will lead to errors in the verification of individual spectral peaks and, as a result, to incorrect estimates of the magnetic parameters of the film.

The aim of this work was to establish the specific features of the angular dependences of the parameters of the microwave curve (H_{res}, ΔH, I) in order to use them in identifying the modes of the recorded spectra.

1. MATERIALS AND METHODS

Single-layer $Fe_{20}Ni_{80}$ films with a thickness of 70 and 140 nm, designated as Py_70 and Py_140, were obtained by thermal evaporation in a vacuum (10^{-6} mm Hg) on glass substrates. The choice of thickness took the ratio between the film thickness and the effective exchange radius into account, which, for the sample material, is ≈100 nm.

The absorption spectra were measured using the equipment of Krasnoyarsk Regional Center of Research Equipment of the Federal Research Center Krasnoyarsk Science Center SB RAS, (spectrometer ELEXSYS E580, Bruker, Germany) in the X-band (resonator pump frequency $f = 9.48$ GHz) with transverse cavity pumping. The sample was placed in the antinode of the alternating magnetic field $h_\sim$ of the cavity. The microwave absorption curves were decomposed using the differentiated Lorentz function. The measurements were performed by changing the direction of the constant magnetic field in the angle θ_H and in the angle φ_H (Fig. 1e). The saturation magnetization M_S was measured with a Lake Shore VSM 8604 vibrating magnetometer.

The uniform precession of the magnetization vector, as experimentally observed under FMR, arises in the absence of pinning of surface spins. The limiting cases for a magneto-isotropic sample in the form of an infinitely thin disk were obtained by Kittel [22]:

$$\begin{aligned} \omega_0/\gamma &= (H_0 - 4\pi M_{\text{eff}})\ (\theta_H = 0^\circ); \\ (\omega_0/\gamma)^2 &= H_0(H_0 + 4\pi M_{\text{eff}})\ (\theta_H = 90^\circ), \end{aligned} \quad (1)$$

where $\gamma = 1.758 \times 10^7$ Hz/Oe is the gyromagnetic ratio and θ_H and φ_H are the polar and azimuthal angles of the external constant bias field H_0. We note that M_{eff} includes, in contrast to the saturation magnetization, various internal effects (internal stresses, pores, inhomogeneities, etc.).

The FMR frequency in the spherical coordinate system [27–29] can be expressed via the total energy E of the magnetic system, taking into account the Landau–Lifshitz equation for the motion of the magnetization M in the polar (θ) and azimuthal (φ) angles, as

$$\omega_0 = \frac{\gamma}{M\sin\theta}\left[\frac{\partial^2 E}{\partial\theta^2}\frac{\partial^2 E}{\partial\varphi^2} - \left(\frac{\partial^2 E}{\partial\theta\partial\varphi}\right)^2\right]^{1/2}. \quad (2)$$

The equilibrium position of the magnetization vector and the free energy density [28] are determined by the following relations:

$$\frac{\partial E}{\partial\phi} = \frac{\partial E}{\partial\theta} = 0; \quad (3)$$

$$\begin{aligned} E = -MH[&\sin\theta\sin\theta_H\cos(\varphi - \varphi_H) \\ &+ \cos\theta\cos\theta_H] + [2\pi M^2 + K_n]\cos^2\theta \\ &+ \frac{K_1}{4}[\sin^4\theta\sin^2 2\varphi + \sin^2 2\theta] \\ &+ \frac{K_2}{16}\sin^2 2\theta\sin^2\theta\sin^2 2\varphi + K_u\sin^2\theta\sin^2(\varphi - \varphi_0), \end{aligned} \quad (4)$$

where K_1 and K_2 are the first and second cubic anisotropy constants, K_n is the constant of perpendicular uniaxial anisotropy, K_u is the uniaxial anisotropy constant in the plane, and φ_0 is the angle that characterizes the direction of the uniaxial anisotropy field in the plane.

By solving the system of equations (2)–(4) numerically, one can find the resonant field H_0 of the uniform mode for arbitrary φ_H and given values of the perpendicular anisotropy field ($2K_n/M_S$) and the in-plane anisotropy field ($2K_u/M_S$).

A nonuniform magnetization distribution over the film thickness in the form of standing exchange spin waves, recorded by the SWR method, is possible if the surface spins are rigidly fixed [24]. The position of the resonant fields of the excited modes under the action of a constant magnetic field and $\theta_H = 0^\circ$ is described by the expression

$$H_n = (\omega_0/\gamma) + 4\pi M_{\text{eff}} - \eta_{\text{eff}}k^2, \quad (5)$$

where $\eta_{\text{eff}} = 2A/M_S$ is the spin-wave stiffness, related to the exchange interaction constant A, and $k = \pi n/d$ is the wavevector, depending on the mode number n and the film thickness d.

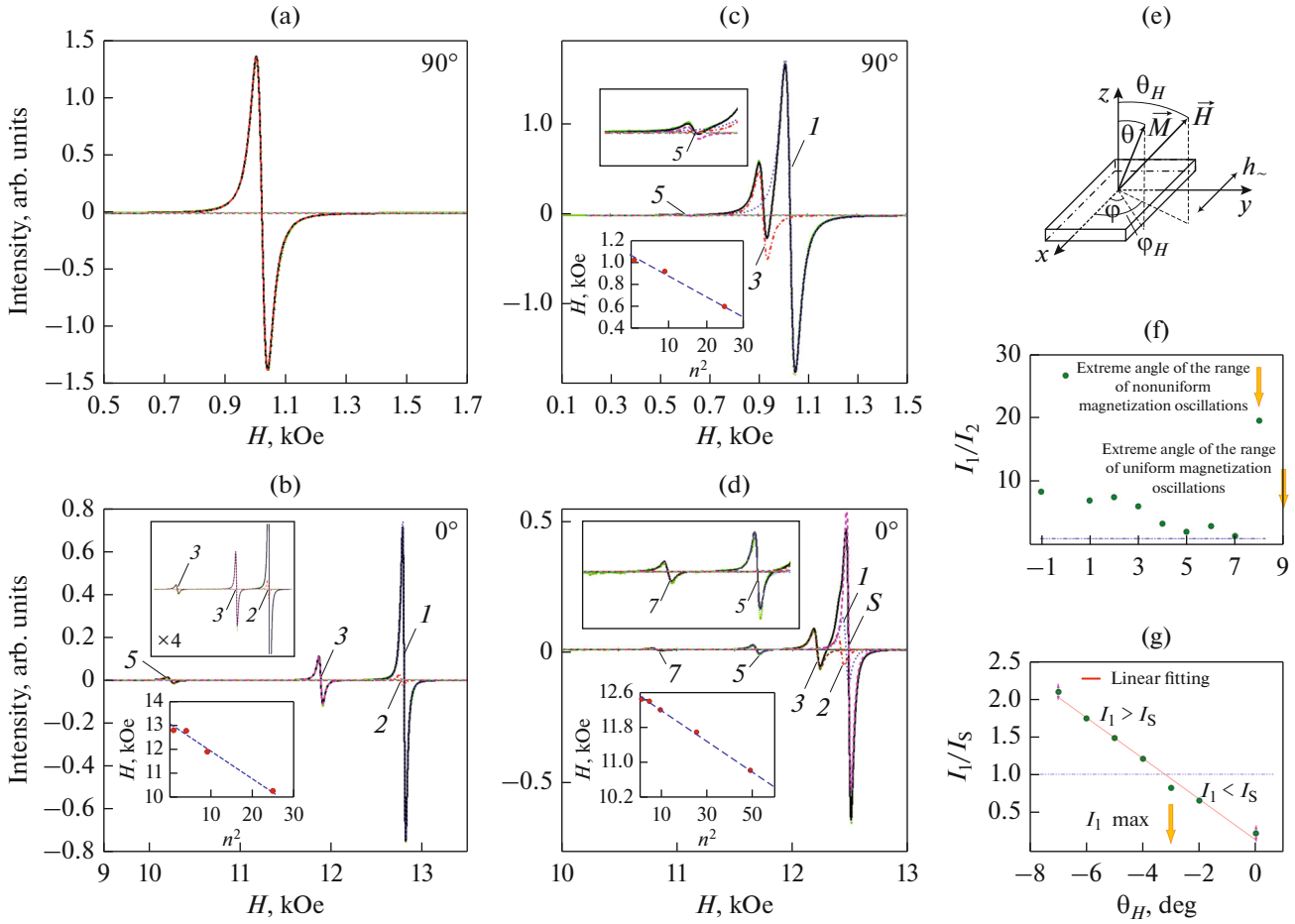

Fig. 1. The experimental microwave spectra for $Fe_{20}Ni_{80}$ single-layer films with a thicknesses of (a, b) 70 and (c, d) 140 nm at (a, c) $\theta_H = 90°$ and (b, d) $\theta_H = 0°$. (d) Schematic geometry of the experiment (e). Intensity ratio of (e) the first and second modes and (f) the first and surface modes at θ_H near 0°. (Insets) Resonant fields vs. squared mode number.

The position of the resonant fields during the recording of the SWR spectrum when $\theta_H = 90°$ [16, 30] is determined as

$$H_n = \left[\sqrt{\left(\frac{\omega_0}{\gamma}\right)^2 + (2\pi M_{\text{eff}})^2} - 2\pi M_S\right] - \eta_{\text{eff}} k^2. \quad (6)$$

Regardless of the geometry of the SWR experiment ($\theta_H = 90°$ or $\theta_H = 0°$), the effective exchange stiffness in the field coordinates is calculated by the formula

$$\tilde{\eta}_{\text{eff}} = (H_1 - H_n)/(n^2 - 1). \quad (7)$$

The realization of some type of magnetization oscillations is determined by the boundary conditions on the film surface [31]. The boundary conditions can be estimated quantitatively and qualitatively from the magnitude and sign of the surface anisotropy constant K_S [26, 32, 33]. If $K_S > 0$ (the easy axis of surface anisotropy is normal to the film surface), then only harmonic SWR modes with real values of the wavevector k are excited. When $K_S < 0$ (the hard axis of surface anisotropy is normal to the film surface), then a hyperbolic nonpropagating exchange spin wave (surface mode) with an imaginary wavevector is also detected in the SWR spectrum. If $K_S = 0$, then a uniform alternating magnetic field $h_\sim$ excites only a uniform magnetization oscillation (FMR) with $k = 0$. According to [24], in the case of symmetric boundary conditions with $K_S = \infty$, the admissible values are $k = \pi n/d$, where $n = 1, 3, 5, 7, \ldots$.

Possible types of absorption spectra were considered in detail in [17]. We note that the surface mode recorded in the SWR spectrum makes it possible to determine the value of K_S:

$$|K_S| = \sqrt{\frac{M_{\text{eff}} A}{2}\left[(H_S - H_1) - \frac{2A}{M_S}\left(\frac{\pi}{d}\right)^2\right]}. \quad (8)$$

The excited standing exchange spin waves recorded in the SWR spectrum in the form of individual peaks

with $k \neq 0$ make it possible to determine the exchange interaction constant A:

$$A = \frac{M_S}{2}\left(\frac{d}{\pi}\right)^2 \frac{H_n - H_{n+1}}{(n+1)^2 - n^2}. \quad (9)$$

It should be noted that the value of A at $\theta_H = 0°$ is the same as at $\theta_H = 90°$.

The angular dependence of the natural nonuniform oscillations of magnetization (standing exchange spin waves) excited under the action of a uniform alternating magnetic field h with a frequency ω is determined by the expression [34]

$$\left(\frac{\omega}{\gamma}\right)^2 = \left(H\sin\theta_H + 4\pi M\sin\theta + \frac{2Ak^2}{M}\sin\theta\right) \times \left(H\sin\theta_H + \frac{2Ak^2}{M}\sin\theta\right) + \left(H\cos\theta_H - 4\pi M\cos\theta + \frac{2Ak^2}{M}\cos\theta\right). \quad (10)$$

The authors of [34] established the uniformity of the angular dependences for the quantity K_S and the function $(\partial H/\partial M)_{\phi,\omega}$. They found that at $\theta_{H\,\mathrm{crit}}$, when $(\partial H/\partial M)_{\phi,\omega} = 0$, a transition occurs from one type of boundary conditions to another. In the first case, $0° < \theta_H < \theta_{H\,\mathrm{crit}}$, there is pinning on the film surfaces and nonuniform modes with $k = \pi n/d$ (SWR) are observed in the microwave spectrum. In the second case, $\theta_{H\,\mathrm{crit}} < \theta_H < 90°$, there is no magnetization pinning on the film surface and an external magnetic field induces uniform oscillations with $k = 0$ (FMR).

2. RESULTS AND DISCUSSION

The angular dependences were measured both in the plane, when the direction of the applied magnetic field varies in the film plane in the angle φ_H, and out of the plane with fixed φ_H and varied θ_H (Fig. 1e). The polar diagrams of the resonant field of the uniform mode for Py_70, as well as the first and third nonuniform modes of the magnetization oscillations for Py_140 at the in-plane orientation, demonstrate the absence of a preferred anisotropy axis in the sample plane.

Examples of experimental microwave spectra in out-of-plane geometry are shown in Fig. 1.

The microwave spectrum of a single-layer FeNi film with a thickness of 70 nm in the range $9° \leq \theta_H \leq 90°$ demonstrates the excitation of a single peak (Fig. 1a), which we identify as a uniform precession mode with $k = 0$. At the same time, in the longitudinal geometry of the experiment, for Py_140, we detected nonuniform precession modes in the form of standing exchange spin waves (Fig. 1c). The absence of a surface mode in the SWR spectrum in the form of an additional peak in fields greater than the field of the main maximum indicates easy axis pinning on each surface of the film. The spectra of Py_140 retain a similar structure and, consequently, similar conditions for pinning on the film surfaces up to $\theta_H = 9°$. The microwave spectra of each of the two films (Figs. 1b and 1d) in the perpendicular geometry of the experiment ($\theta_H = 0°$) demonstrate several well-defined peaks caused by the excitation of exchange standing spin waves. The spectrum of Py_140, in addition to standing waves, contains a damped surface mode in fields greater than the first bulk mode, which indicates that the easy plane boundary conditions occur on one of the film surfaces.

The positions of the resonant fields H_n of nonuniform modes in the SWR spectra of the samples are described by linear dependences on the squared mode number, irrespective of the experiment geometry (Fig. 1e). The assumption that the SWR spectrum is recorded over the entire range of angles θ_H for Py_140 is confirmed by the fairly close values of the effective exchange stiffness (in field units (7)) of 27 ± 1.5 and 24 ± 1.5 Oe at 0° and 90°, respectively.

The identification of individual peaks near $\theta_H = 90°$ was carried out taking the intensity ratio of the neighboring peaks as a function of the angle θ_H into account. First, it is worth noting the predominance of the intensity of the surface mode I_S over the intensity of the first exchange mode I_1 for Py_140 [26, 32, 33].

Second, the intensity ratio of two bulk modes must depend on the angle weakly, while the intensity ratio of the surface and first bulk modes critically depends on the angle (Figs. 1f and 1g). The change of the relation $I_S > I_1$ to $I_S < I_1$ is due to a gradual decrease in the contribution of the boundary conditions to the formation of magnetization waves over the film thickness upon deviation from $\theta_H = 0°$.

Third, the functional dependences of the intensity ratios of the nearest modes on the angle differ depending on their distribution over the film (Figs. 1f and 1g).

The ratio I_1/I_S increases linearly with an increase in the angle between an external field and the normal to the film plane (Fig. 1g), and I_1/I_2 exhibits extremum points at $\theta_H = 0°$ and $\theta_H = \theta_{H\,\mathrm{crit}}$ (Fig. 1f), where $\theta_{H\,\mathrm{crit}}$ is the critical angle at which the oscillation mode changes from uniform to nonuniform.

The angular dependences of the parameters of the first standing mode or the uniform peak of the films under study are shown in Fig. 2. Changes in the type of oscillations from uniform (FMR) to nonuniform (SWR) for the Py_70 sample were detected simultaneously according to two features: the structure of the recorded spectrum (appearance of additional peaks in the range of angles $-8° \leq \theta_H \leq 8°$) and a change in the angular dependence of the intensity of the largest recorded peak at $\theta_H = 8°$ (Fig. 2c). It should by noted that the transition from some pinning conditions to others at finite values of the surface pinning constant,

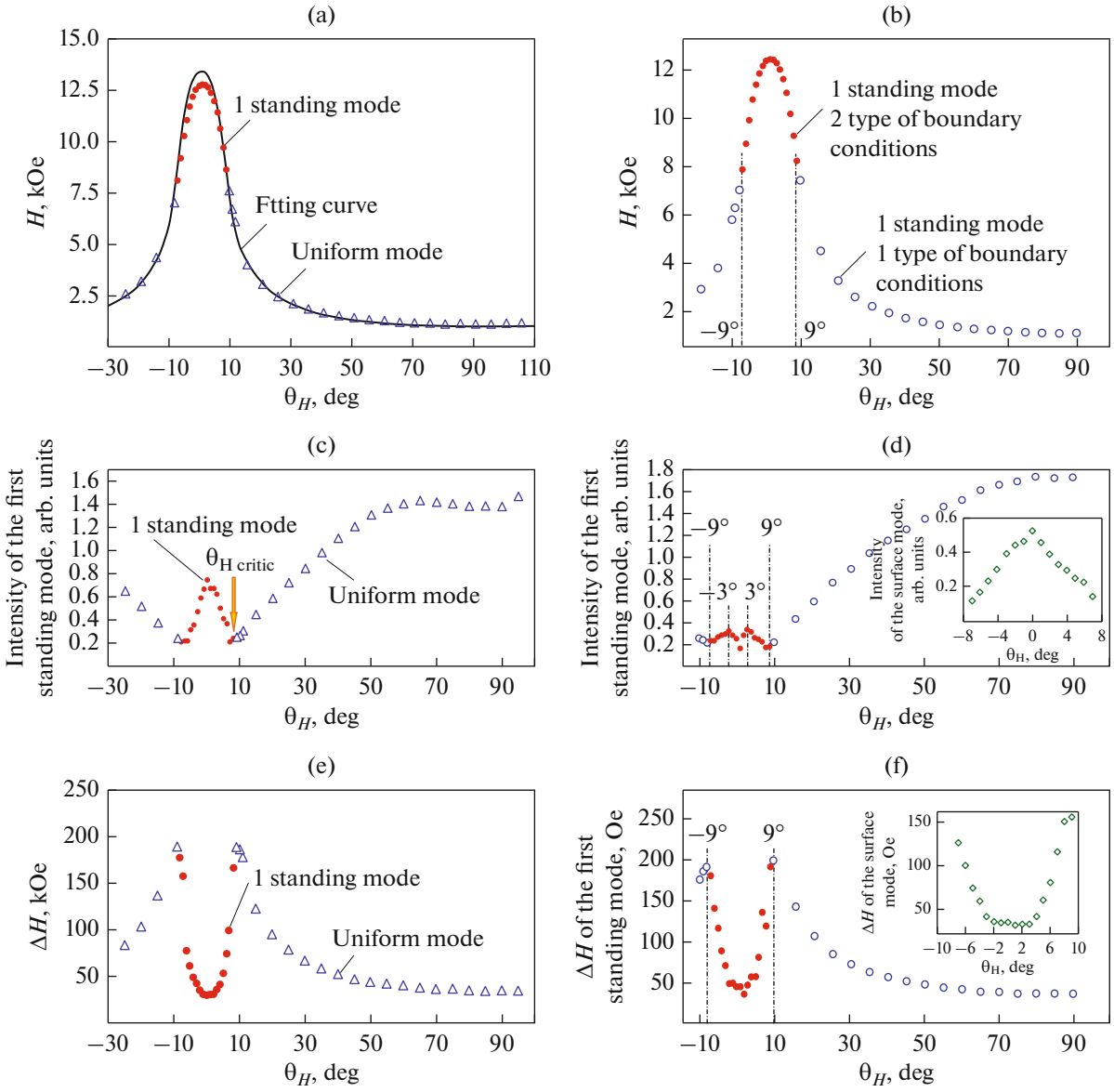

Fig. 2. The angular dependences of (a, b) H_{res}, (c, d) I, and (e, f) ΔH for (a, c, e) Py_70 and (b, d, f) Py_140 films. (Insets) Angular dependences of the surface mode.

which is observed for Py_140, is also accompanied by a change in the angular dependence of the intensity of the first standing exchange mode. Comparison of the angular dependences of the intensities of the first bulk modes of Py_70 and Py_140 in the range of angles $-8° \le \theta_H \le 8°$ reveals the effect of the easy-plane boundary conditions on the intensity of the first bulk mode. The absence of surface peaks in the microwave spectrum of the Py_70 film is indicative of the easy-axis boundary conditions on both surfaces, and the intensity of the first bulk mode reaches a maximum at $\theta_H = 0°$. The easy-plane surface anisotropy occurs on one of the surfaces of the Py_140 film with a perpendicular geometry of the experiment, and the most intense peak at $\theta_H = 0°$ is due to the surface wave; extrema of the first bulk mode are observed at $\theta_H = 3°$ and $\theta_H = -3°$ (Fig. 2).

The angular dependences of the linewidth should be estimated taking the ratio $(\omega/\gamma)/4\pi M_S$ into account [35, 36]. The authors of [35] studied the resonant curves calculated from (2)–(4) at different fixed frequencies of the cavity and noted that, in the case of $(\omega/\gamma)/4\pi M_S \sim 0.1$ and at θ_H in the range 2°–10°, a false increase in ΔH is observed. This effect is due to the shape anisotropy. Taking the fact into account that the ratio $(\omega/\gamma)/4\pi M_S$ for our systems is close to 0.1, we believe that the "physical" absorption linewidth ΔH for both Py_70 and Py_140 does not depend on θ_H

Table 1. The magnetic parameters

Sample		M_{eff}, G	$A \times 10^{-6}$, erg/cm	K_S, erg/cm^2
Py_70		812 ± 20	0.23 ± 0.02	–
Py_140	$\theta_H = 0°$	750 ± 15	0.26 ± 0.02	0.024
	$\theta_H = 90°$		0.16 ± 0.02	–

and, when estimating ΔH for calculating the relaxation parameter, the boundary values of the angular range should be used. The value of physical ΔH at θ_H equal to 0° and 90° is ~30 Oe for Py_70 and ~40 Oe for Py_140. At the same time, the shape of the $\Delta H(\theta_H)$ curve is of qualitative interest and allows one to determine the critical angles θ_H from the extremum points.

Taking the perpendicular anisotropy field in expressions (2)–(4) equal to –100 Oe, we calculated the fitting curve for the Py_70 sample, which coincides quite accurately with the positions of the experimental resonant fields of the uniform mode (the relative error in the field magnitude is within 5%) (Fig. 2a). The value of M_S used in the calculation of the fitting curve was 820 ± 20 G and was measured on a vibrating magnetometer.

The values of H_{res}, ΔH, and I made it possible to determine the exchange interaction constant A, the surface anisotropy constant K_S, and the effective magnetization M_{eff} (Table 1).

The angular dependence of the peak intensity (Figs. 2c and 2d) makes it possible to estimate the critical angle θ_H at which either the oscillation type changes from uniform to nonuniform ($\theta_H \approx 8°$ for Py_70) or the boundary conditions for the pinning ($\theta_H \approx 8°$ for Py_140) change.

CONCLUSIONS

The angular dependence of the intensity of the detected peak of the microwave curve allows one to accurately determine the type of oscillation: uniform or nonuniform (surface or bulk standing mode). The intensity ratio of two adjacent peaks in the case of a slight difference in the magnitude of their resonant fields can be used to identify surface (hyperbolic) and bulk (trigonometric) nonuniform magnetization oscillations. In the first case, when comparing the intensities of two adjacent bulk modes, no change in the sign of the ratio occurs: the mode with a smaller wavenumber k in the range of angles at which nonuniform oscillations occur has a higher intensity and the ratio I_k/I_{k+1} is greater than unity. In the second case, when comparing the intensities of the surface mode and the first bulk standing mode, a reversal of sign of the ratio is observed: $I_S > I_1$ changes to $I_S < I_1$ after some critical angle $\theta_{H\,crit}$. It is also worth noting the linear dependence of I_1/I_S on the angle θ_H.

It has been found that the angle $\theta_{H\,crit}$ at which the oscillation type changes from uniform to nonuniform corresponds to an extremum (minimum) point of the angular dependence of the intensity. The shape of the dependence $I(\theta_H)$ reflects the type of the surface conditions at the film boundaries. The intensity of the first standing exchange mode, when the pinning on each surface of the film is easy-axis, gradually increases in the range of angles from $\theta_{H\,crit}$ to 0° (or decreases in the range of angles from 0° to $\theta_{H\,crit}$) and is characterized by a maximum value at $\theta_H = 0°$. The dependence $I(\theta_H)$ where at least on one surface of the film, easy-plane pinning occurs, has a minimum of I_1 at $\theta_H = 0°$ and the maximum of I_1 located symmetrically with respect to $\theta_H = 0°$.

Thus, the angular dependences of the resonant field, intensity, and linewidth, along with the structure of the microwave spectra, reflect both the change in the oscillation type from uniform to nonuniform and the type of surface pinning. The characteristics of the angular dependences of the parameters of the detected peaks of the microwave spectrum contribute to the accurate verification of the spectra and, as a result, the correct determination of both bulk and surface parameters of a magnetic system.

CONFLICT OF INTEREST

The authors declare that they have no conflicts of interest.

REFERENCES

1. V. V. Kruglyak, C. S. Davies, V. S. Tkachenko, O. Y. Gorobets, Y. I. Gorobets, and A. N. Kuchko, "Formation of the band spectrum of spin waves in 1D magnonic crystals with different types of interfacial boundary conditions," J. Phys. D: Appl. Phys. **50**, 094003 (2017).
2. A. I. Stognij, L. V. Lutsev, V. E. Bursian, and N. N. Novitskii, "Growth and spin-wave properties of thin $Y_3Fe_5O_{12}$ films on Si substrates," J. Appl. Phys. **118**, 023905 (2015).
3. R. S. Iskhakov, S. V. Stolyar, M. V. Chizhik, and L. A. Chekanova, "Spin-wave resonance in multilayer films (one-dimensional magnon crystals). Identification rules," JETP Lett. **94**, 301–305 (2011).
4. D. M. Jacobi, E. Sallica Leva, N. Álvarez, M. Vásquez Mansilla, J. Gómez, and A. Butera, "Angular and frequency dependence of standing spin waves in FePt films," J. Appl. Phys. **111**, 033911 (2012).
5. S. V. Stolyar, V. Y. Yakovchuk, I. G. Vazhenina, and R. S. Iskhakov, "Study of surface anisotropy of the interface of two-layer DyCo/FeNi films by the spin-wave resonance method," J. Supercond. Nov. Magn. **34**, 2969–2975 (2021).
6. R. S. Iskhakov, S. V. Stolyar, L. A. Chekanova, and I. G. Vazhenina, "Spin-wave resonance in exchange-

coupled three-layer FeNi/Cu/FeNi planar structures," Fiz. Tv. Tela **62**, 1658–1664 (2021).

7. G. Thirupathi and R. Singh, "Structural and FMR line shape analysis of Mn Zn-ferrite nanoparticles," AIP Conf. Proc. **1665**, 050133 (2015).
8. L. A. Chekanova, S. V. Komogortsev, E. A. Denisova, L. A. Kuzovnikova, I. V. Nemtsev, R. N. Yaroslavtsev, and R. S. Iskhakov, "Ferromagnetic resonance linewidth in powders consisting of core–shell particles," Bull. Russ. Acad. Sci.: Phys. **81**, 380–382 (2017).
9. L. Dreher, C. Bihler, E. Peiner, A. Waag, W. Schoch, W. Limmer, S. T. B. Goennenwein, and M. S. Brandt, "Angle-dependent spin-wave resonance spectroscopy of (Ga,Mn)As films," Phys. Rev. B **87**, 224422 (2013).
10. A. I. Dmitriev, R. B. Morgunov, O. L. Kazakova, and Y.Tanimoto, "Spin-wave resonance in Ge_{1-x} Mn_x films exhibiting percolation ferromagnetism," J. Exp. Theor. Phys **108**, 985–991 (2009).
11. X. Liu and J. K. Furdyna, "Ferromagnetic resonance in $Ga_{1-x}Mn_xAs$ dilute magnetic semiconductors," J. Phys. Condens. Matter **18**, R245–R279 (2006).
12. A. Butera, J. N. Zhou, and J. A. Barnard, "Ferromagnetic resonance in as-deposited and annealed Fe–SiO_2 heterogeneous thin films," Phys. Rev. B **60**, 12270–12278 (1999).
13. E. A. Denisova, S. V. Komogortsev, R. S. Iskhakov, L. A. Chekanova, A. D. Balaev, Y. E. Kalinin, and A. V. Sitnikov, "Magnetic anisotropy in multilayer nanogranular films $(Co_{40}Fe_{40}B_{20})_{50}(SiO_2)_{50}$/α-Si:H," J. Magn. Magn. Mater. **440**, 221–224 (2017).
14. D. A. Balaev, A. A. Krasikov, A. A. Dubrovskiy, S. I. Popkov, S. V. Stolyar, O. A. Bayukov, R. S. Iskhakov, V. P. Ladygina, and R. N. Yaroslavtsev, "Magnetic properties of heat treated bacterial ferrihydrite nanoparticles," J. Magn. Magn. Mater. **410**, 171–180 (2016).
15. S. V. Stolyar, R. N. Yaroslavtsev, R. S. Iskhakov, O. A. Bayukov, D. A. Balaev, A. A. Dubrovskii, A. A. Krasikov, V. P. Ladygina, A. M. Vorotynov, and M. N. Volochaev, "Magnetic and resonance properties of ferrihydrite nanoparticles doped with cobalt," Phys. Solid State **59**, 555–563 (2017).
16. R. S. Iskhakov, V. A. Seredkin, S. V. Stolyar, L. A. Chekanova, and V. Yu. Yakovchuk, "Spin-wave resonance in three-layer NiFe/Dy_xCo_{1-x}/NiFe films as a method for detecting structural inhomogeneities in amorphous Dy_xCo_{1-x} layers," JETP Lett. **76**, 779–783 (2002).
17. I. G. Vazhenina, R. S. Iskhakov, and L. A. Chekanova, "Spin-wave resonance in chemically deposited Fe–Ni films: measuring the spin-wave stiffness and surface anisotropy constant," Phys. Solid State **60**, 292–298 (2018).
18. H. Puszkarski and P. Tomczak, "Spin-wave resonance as a tool for probing surface anisotropies in ferromagnetic thin films: Application to the study of (Ga,Mn)As," Surf. Sci. Rep. **72**, 351–367 (2017).
19. E. K. Zavoiskii, "Magneto-spin resonance in ferromagnets at centimeter wavelengths," Zh. Eksp. Tekh. Fiz. **17**, 883–888 (1947).
20. J. H. E. Griffiths, "Anomalous high-frequency resistance of ferromagnetic metals," Nature **158**, 670–671 (1946).
21. C. Kittel, "Interpretation of anomalous Larmor frequencies in ferromagnetic resonance experiment," Phys. Rev. **71**, 270–271 (1947).
22. C. Kittel, "On the theory of ferromagnetic resonance absorption," Phys. Rev. **73**, 155–161 (1948).
23. M. H. Seavey and P. E. Tannenwald, "Direct observation of spin-wave resonance," Phys. Rev. Lett. **1**, 168–169 (1958).
24. C. Kittel, "Excitation of spin waves in a ferromagnet by a uniform rf field," Phys. Rev. **110**, 1295–1297 (1958).
25. W. S. Ament and G. T. Rado, "Electromagnetic effects of spin wave resonance in ferromagnetic metals," Phys. Rev. **97**, 1558–1566 (1955).
26. Yu. A. Korchagin, R. G. Khlebopros, and N. S. Chistyakov, "Spin-wave resonance in magnetic films with additional surface layers," Fiz. Met. Metalloved. **34**, 1303–1305 (1972).
27. H. Suhl, "Ferromagnetic resonance in nickel ferrite between one and two kilomegacycles," Phys. Rev. **97**, 555–557 (1955).
28. J. Smit and H. G. Beljers, "Ferromagnetic resonance absorption in $BaFe_{12}O_{12}$, a highly anisotropic crystal," Philips Res. Rep. **10**, 113–130 (1955).
29. J. O. Artman, "Ferromagnetic resonance in metal single crystals," Phys. Rev. **105**, 74–84 (1957).
30. M. Nisenoff and R. W. Terhune, "Experimental studies of standing spin-wave modes in ferromagnetic films," J. Appl. Phys. **35**, 806–807 (1964).
31. J. T. Yu, R. A. Turk, and P. E. Wigen, "Exchange-dominated surface spin waves in thin yttrium-iron-garent films," Phys. Rev. B **11**, 420–434 (1975).
32. Yu. A. Korchagin, R. G. Khlebopros, and N. S. Chistyakov, "Spin-wave resonance spectrum in a thin ferromagnetic layer with mixed boundary conditions," Fiz. Tverd. Tela **14**, 2121–2123 (1972).
33. N. M. Salanskii and M. Sh. Erukhimov, *Physical Properties and Application of Magnetic Films* (Nauka, Novosibirsk, 1975) [in Russian].
34. P. E. Wigen, C. F. Kooi, M. R. Shanabarger, U. K. Cummings, and M. E. Baldwin, "Angular dependence of spin pinning in thin ferromagnetic films," J. Appl. Phys. **34**, 1137–1139 (1963).
35. P. E. Tannenwald and M. H. Seavey, "Ferromagnetic resonance in thin films of permalloy," Phys. Rev. **105**, 377–378 (1957).
36. K. Zakeri, J. Lindner, I. Barsukov, R. Meckenstock, M. Farle, U. von Horsten, H. Wende, W. Keune, J. Rocker, S. S. Kalarickal, K. Lenz, W. Kuch, K. Baberschke, and Z. Frait, "Spin dynamics in ferromagnets: Gilbert damping and two-magnon scattering," Phys. Rev. B **76**, 104416 (2007).

Translated by E. Chernokozhin